Title

Immune Reconstitution Bone Loss Exacerbates Bone Degeneration Due to Natural Aging in a Mouse Model

Journal

The Journal of Infectious Diseases, 226(1)

ISSN

0022-1899

Authors

Weitzmann, M Neale
Weiss, Daiana
Vikulina, Tatyana
et al.

Publication Date

2022-08-12

DOI

10.1093/infdis/jiab631

Peer reviewed

The Journal of Infectious Diseases

MAJOR ARTICLE

Immune Reconstitution Bone Loss Exacerbates Bone Degeneration Due to Natural Aging in a Mouse Model

M. Neale Weitzmann,[1,2,a] Daiana Weiss,[2,b] Tatyana Vikulina,[1,2,b] Susanne Roser-Page,[1] Kanglun Yu,[3] Meghan E. McGee-Lawrence,[3,4] Chia-Ling Tu,[5] Wenhan Chang,[5] and Ighovwerha Ofotokun[6,7,a]

[1]Atlanta Department of Veterans Affairs Medical Center, Decatur, Georgia, USA, [2]Division of Endocrinology, Metabolism, and Lipids, Department of Medicine, Emory University School of Medicine, Atlanta, Georgia, USA, [3]Department of Cellular Biology and Anatomy, Medical College of Georgia, Augusta University, Augusta, Georgia, USA, [4]Department of Orthopaedic Surgery, Medical College of Georgia, Augusta University, Augusta, Georgia, USA, [5]Endocrine Research Unit, San Francisco VA Healthcare System, University of California, San Francisco, California, USA, [6]Division of Infectious Diseases, Department of Medicine, Emory University School of Medicine, Atlanta, Georgia, USA, [7]Grady Healthcare System, Atlanta, Georgia, USA

Background. Immune reconstitution bone loss (IRBL) is a common side-effect of antiretroviral therapy (ART) in people with human immunodeficiency virus (PWH). Immune reconstitution bone loss acts through $CD4^+$ T-cell/immune reconstitution-induced inflammation and is independent of antiviral regimen. Immune reconstitution bone loss may contribute to the high rate of bone fracture in PWH, a cause of significant morbidity and mortality. Although IRBL is transient, it remains unclear whether bone recovers, or whether it is permanently denuded and further compounds bone loss associated with natural aging.

Methods. We used a validated IRBL mouse model involving T-cell reconstitution of immunocompromised mice. Mice underwent cross-sectional bone phenotyping of femur and/or vertebrae between 6 and 20 months of age by microcomputed tomography (μCT) and quantitative bone histomorphometry. $CD4^+$ T cells were purified at 20 months to quantify osteoclastogenic/inflammatory cytokine expression.

Results. Although cortical IRBL in young animals recovered with time, trabecular bone loss was permanent and exacerbated skeletal decline associated with natural aging. At 20 months of age, reconstituted $CD4^+$ T cells express enhanced osteoclastogenic cytokines including RANKL, interleukin (IL)-1β, IL-17A, and tumor necrosis factor-α, consistent with elevated osteoclast numbers.

Conclusions. Immune reconstitution bone loss in the trabecular compartment is permanent and further exacerbates bone loss due to natural aging. If validated in humans, interventions to limit IRBL may be important to prevent fractures in aging PWH.

Keywords. aging; antiretroviral therapy; HIV; immune reconstitution bone loss; T cells.

Although antiretroviral therapy (ART) has dramatically extended the lifespan of people with human immunodeficiency virus (PWH), comorbidities are now common and account for more than half the deaths observed among PWH [1].

Human immunodeficiency virus (HIV) infection is itself a risk factor for low bone mineral density (BMD) [2–8], and this bone loss is compounded by BMD reductions of up to 6% within the first 6–48 months of ART initiation [9–13], leading to significantly increased fracture risk in PWH [14–19].

Immune reconstitution bone loss is an unavoidable side-effect of ART, driven by $CD4^+$ T-cell reconstitution and adaptive immune system reactivation [20, 21], and consequently occurs independently of the specific type of antiviral regimen [22–26]. Indeed, bone resorption and loss correlates significantly with the magnitude of $CD4^+$ T-cell reconstitution [26] and with baseline $CD4^+$ T-cell number [26, 27].

To study the mechanisms of IRBL, we developed a mouse model involving adoptive transfer of T cells into T cell-deficient TCRβ knockout (KO) mice [28] to mimic T-cell homeostatic repopulation after ART in humans. It is remarkable that T-cell reconstitution mirrored all major features of human IRBL after ART, establishing a platform to further study the mechanisms driving IRBL [28, 29].

Because fracture risk increases significantly with age in both general populations and in PWH [14], there is now concern that IRBL may compound bone loss due to natural aging and lead to increased fracture incidence in PWH. Indeed, of the 1.3 million PWH in the United States, 50% are over the age of 50, and it is estimated that 70% will be over the age of 50 by 2030 [30].

In the present study, we used our IRBL mouse model to investigate the hypothesis that IRBL causes irreparable damage to the skeleton, which is further exacerbated by the bone loss associated with natural aging.

MATERIALS AND METHODS

Mice

Animal studies were approved by the Emory Institutional Animal Care and Use Committee. All studies used female, wild-type (WT)

Received 2 September 2021; editorial decision 21 December 2021; accepted 23 December 2021; published online 28 December 2021.

[a]M. N. W. and I. O. contributed equally as lead authors.

[b]T. V. and D. W. contributed equally to the experimental execution of the work.

Correspondence: M. Neale Weitzmann, PhD, Division of Endocrinology, Metabolism, and Lipids, Emory University School of Medicine, 101 Woodruff Circle, 1305 WMRB, Georgia (mweitzm@emory.edu).

The Journal of Infectious Diseases® 2022;226:38–48

https://doi.org/10.1093/infdis/jiab631

C57BL6/J mice and T cell-deficient TCRβ KO mice (Jackson Laboratory, Bar Harbor, ME). Mice were housed under specific pathogen-free conditions and fed gamma-irradiated 5V5R mouse chow (LabDiet, St. Louis, MO) and water ad libitum.

T-Cell Adoptive Transfer

Immune reconstitution bone loss was induced as previously described [28, 29] by syngeneic adoptive transfer of 1×10^5 immunomagnetically purified (StemCell Technologies, Cambridge, MA) splenic $CD3^+$ T cells, from 6-month-old female WT mice, into 6 month-old TCRβ KO mice by tail-vein injection. Sham controls were injected with vehicle (phosphate-buffered saline). Mice were sacrificed for immunoskeletal profiling 3 months after reconstitution (9 month of age) as previously described [28]. Nine months of age represents adult humans 30–38 years of age [31]. Mice were also killed at 14 months of age (considered "middle age" in mice and representing humans of ~50 years of age) and at 20 months of age (considered "old" in mice, with senescent changes present in almost all biomarkers and representative of older humans between 56 and 69 years of age [31]). Untransplanted TCRβ KO mice 6 months of age were used as a baseline control.

Microcomputed Tomography

Microcomputed tomography (μCT) was performed, as previously described [28, 32], in vertebrae and femurs ex vivo using a μCT40 scanner (Scanco Medical, Wangen-Brüttisellen, Switzerland). For trabecular bone, 200 tomographic slices were taken (total area = 1200μm) at the distal right femoral metaphysis or the L3 vertebrae, at a voxel size of 6 μm (70 kVp and 114 mA, and 200 ms integration time). Cortical bone was quantified at the mid-diaphysis from 99 slices at a voxel size of 6 μm (total area = 594 μm).

Quantitative Bone Histomorphometry

Bone histology and histomorphometric analysis was performed at Augusta University, as previously described [33], using (BioquantOsteo, Nashville, TN) software, on undecalcified and unstained double calcein-labeled (7-day interval) femoral sections for dynamic bone formation and tartrate-resistant acid phosphatase (TRAP)-stained sections for osteoclasts. Images were captured on an Olympus IX70 (Olympus Life Science, Waltham, MA).

Biochemical Indices of Bone Turnover

Mice were killed by exsanguination using cardiac puncture under isoflurane anesthesia for serum collection. C-terminal telopeptide of type I collagen (CTx), osteocalcin, total soluble receptor activator of NF-κB ligand (RANKL), osteoprotegerin (OPG), and tumor necrosis factor (TNF)α were quantified in serum using commercial enzyme-linked immunosorbent assays from Immunodiagnostic Systems Inc. (Gaithersburg, MD) and from R&D Systems (Minneapolis, MN) for RANKL, OPG, and TNFα.

NanoString Expression Profiling

Expression of RANKL, OPG, TNFα, interleuking (IL)-1β, IL-17A, and IL-6 messenger ribonucleic acid (mRNA) was quantified from 50 000 immunomagnetically purified (StemCell Technologies) $CD4^+$ T cells lysed directly in 1:3 RLT buffer (QIAGEN, Germantown, MD) and hybridized with gene-specific fluorescent barcoded probes at 65°C for 24 hours without RNA extraction. The mRNA was quantified on an nCounter Max analysis system, and transcripts were normalized to β-Actin, β_2-microglobulin, and Gilz, using nSolver 4.0 software (NanoString Technologies, Seattle, WA).

Statistical Analysis

Statistical significance was determined using GraphPad Prizm8.4.3 for Mac (GraphPad Software Inc., La Jolla, CA). Normal distribution was assessed by Shapiro-Wilk test. Multiple comparisons were analyzed by 2-way analysis of variance (ANOVA) with Bonferroni correction. Simple group comparisons involved unpaired Student's *t* test for parametric data or Mann-Whitney test for non-parametric data. All tests were 2-sided and $P < .05$ was considered a statistically significant result. Line data are expressed as mean ± standard error of the mean, and boxplots represent median ± interquartile range with 10–90 percentile whiskers.

RESULTS

Trabecular Bone Mass Is Permanently Diminished by Immune Reconstitution and Is Cumulative With Age-Associated Bone Loss

Using high-resolution (6 μm) μCT, we analyzed the L3-lumbar vertebrae and distal-femoral metaphasis of T-cell reconstituted (T cells) and sham mice at 6, 9, 14, and 20 months of age.

Two-way ANOVA revealed significant effects of time ($P < .0001$) and T-cell reconstitution ($P < .0001$) on vertebral bone volume fraction (bone volume), the key index of trabecular bone mass (Figure 1A). However, interaction between time and T cells fell short of statistical significance ($P = .0841$). Vertebral bone volume in sham mice declined significantly ($P = .0036$) between 6 and 20 months of age, which is indicative of aging bone loss.

Vertebral bone volume was significantly diminished due to IRBL in T-cell reconstituted mice, with respect to sham, at 9 months of age and remained significantly lower than sham groups at 14 months of age, reaching a percentage change difference of −27.4% by 20 months of age (Figure 1A), indicating a cumulative effect of IRBL and aging-bone loss.

Bone volume reflects total trabecular microarchitecture, represented by trabecular number, thickness, and separation. Significant effects of time ($P < .0001$) and T-cell reconstitution ($P < .0001$) were observed for trabecular number and trabecular separation as well as significant interactions between time and T cells ($P = .0268$ and $P = .0134$ for number and separation, respectively). Trabecular thickness likewise showed a significant effect of time ($P < .0001$) and interaction between T cells

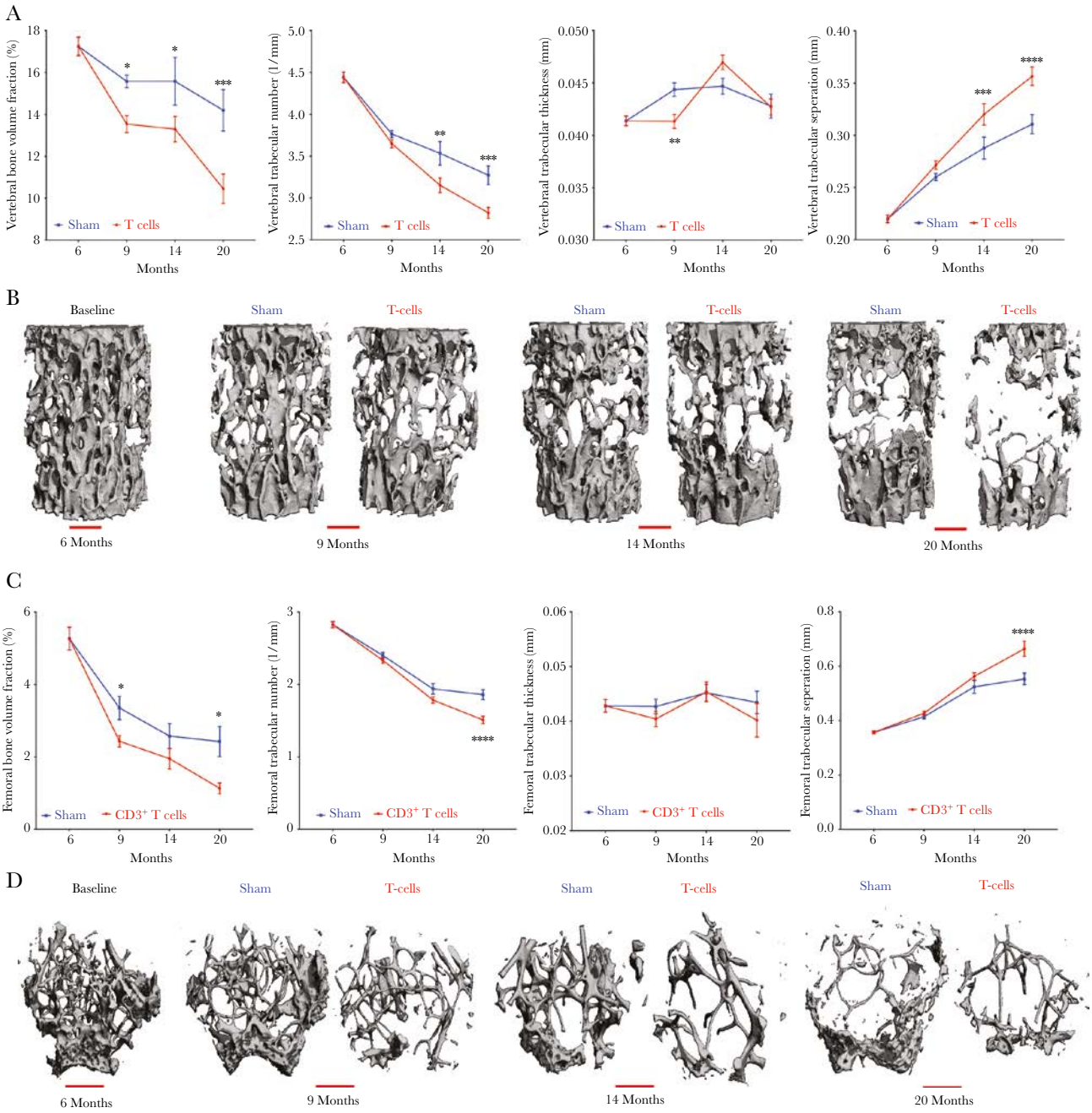

Figure 1. Microcomputed tomography (μCT) analysis of lumbar vertebrae and femoral trabecular bone in sham-reconstituted (Sham) and T-cell reconstituted (T cells) mice. Six-month-old female C57BL6/J TCRβ knockout (KO) mice were sham-reconstituted or T-cell reconstituted by adoptive transfer with 1×10^5 $CD3^+$ T cells, and changes in trabecular bone structure and mass were quantified in L3 vertebrae and distal femoral metaphysis, by high-resolution (6 μm) μCT, in cross-sectional groups at 6, 9, 14, and 20 months of age. (A) Vertebral and (C) femoral trabecular indices are shown for bone volume fraction, trabecular number, trabecular thickness, and trabecular separation. Data are expressed as mean ± standard error of the mean: $*P < .05$, $**P < .01$, $***P < .001$, and $****P < .0001$ for T-cell compared with sham by 2-way analysis of variance with Bonferroni posttest. Nonsignificant comparisons not shown. n = 12 mice/group at 6 months, 22–23 mice/group at 9 months, 15–16 mice/group at 14 months, and 15–16 mice/group at 20 months. Representative high-resolution (6 μm) 3-dimensional reconstructions of (B) L3 vertebrae and (D) distal femur for sham and reconstituted (T cell) mice are shown for baseline (6 months) and 9 months, 14 months, and 20 months. Scale bars represent 500 μm.

and time ($P = .0030$); however, there was no significant overall effect of T-cell reconstitution itself.

Trabecular number was diminished between sham and T-cell groups at 14 and 20 months of age, whereas trabecular separation was increased (Figure 1A), consistent with diminished bone volume. Trabecular number was not affected by IRBL (9 months of age), instead IRBL was associated with diminished trabecular thickness.

The data suggest that although bone volume decline associated with IRBL was driven primarily by a decline in trabecular

thickness, bone volume declines due to aging were driven primarily by a decline in trabecular number. Representative 3-dimensional reconstructions of vertebral trabecular bone are shown in Figure 1B.

Similar changes in bone volume were observed in the trabecular compartment of the distal femur (Figure 1C). Like the axial skeleton, 2-way ANOVA revealed statistically significant main effects of time ($P < .0001$) and T-cell reconstitution ($P = .0010$) on femoral bone volume but no significant interaction between time and T-cell reconstitution.

Femoral bone volume was significantly ($P = .0435$) diminished in the first 3 months by T-cell reconstitution, relative to sham control. Sham mice further lost significant ($P < .0001$) amounts of bone volume between 6 and 20 months of age, consistent with natural aging bone loss. T-cell reconstituted mice had significantly ($P = .0102$) reduced percentage change difference in bone volume of −53.3% relative to sham controls at 20 months of age. These data suggest that, as in the vertebrae, trabecular IRBL in the femur was cumulative with bone loss due to natural aging.

Significant effects of time ($P < .0001$ and $P < .0001$), T-cell reconstitution ($P = .0002$ and $P = .0007$), and interaction between time and T-cell reconstitution ($P = .0047$ and $P = .0096$) were observed for trabecular number and separation, respectively. There were no significant differences for trabecular thickness.

Femoral trabecular number, but not trabecular thickness, was significantly ($P < .0001$) lower and trabecular separation was significantly ($P < .0001$) higher in T-cell reconstituted groups compared with sham controls at 20 months of age (Figure 1C), indicative of diminished bone structure. Representative 3-dimensional reconstructions of femoral trabecular bone are shown in Figure 1D.

Cortical Bone Volume Is Transiently Diminished by Immune Reconstitution in Skeletally Mature Mice but Recovers Before Onset of Age-Associated Bone Loss

In the cortical compartment of the femur, 2-way ANOVA revealed statistically significant main effects of (1) time ($P = .0015$) and T-cell reconstitution ($P = .0076$) on cortical thickness and (2) time ($P < .0001$) and T-cell reconstitution ($P = .0123$) on cortical area, 2 key indices of cortical bone mass. Neither index revealed a significant interaction between time and T-cell reconstitution (Figure 2A).

In contrast to the trabecular bone compartment, by 9 months of age (3 months after T-cell reconstitution) cortical thickness and cortical area were significantly reduced by IRBL in T-cell reconstituted mice (Figure 2A). Cortical bone loss was transient, however, and not significantly different between groups at 14 and 20 months of age for either cortical thickness or area

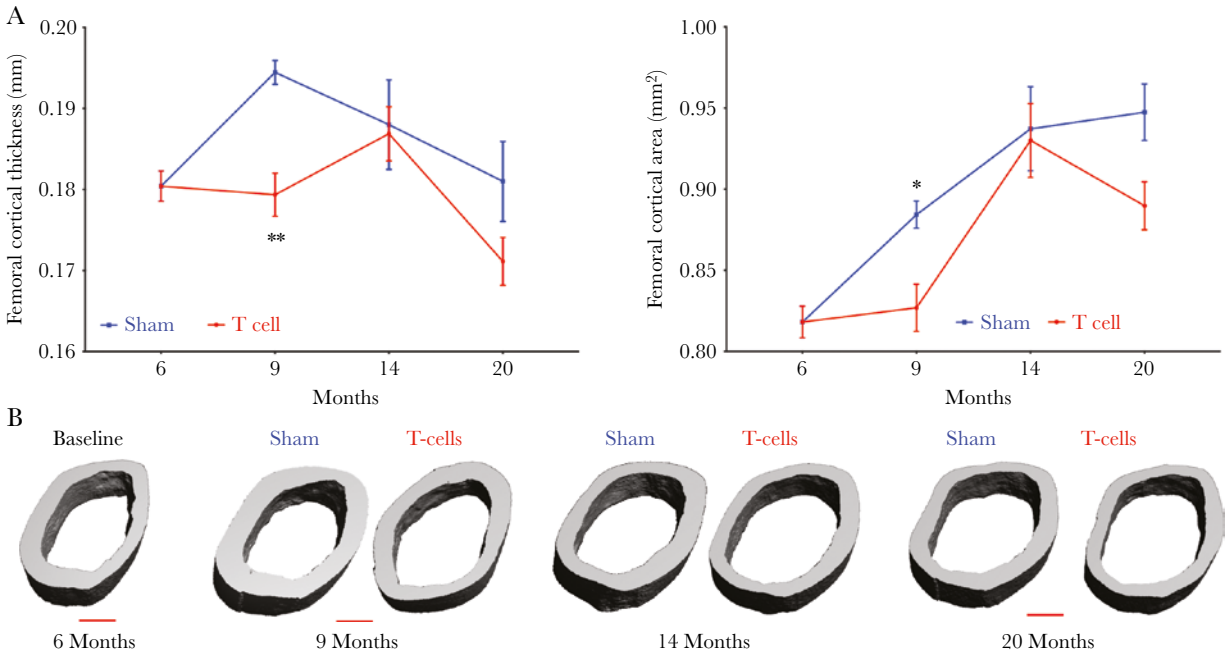

Figure 2. Microcomputed tomography (μCT) analysis of femoral cortical bone in sham-reconstituted (Sham) and T-cell reconstituted (T cells) mice. Six-month-old female TCRβ knockout (KO) mice were sham-reconstituted or T-cell reconstituted by adoptive transfer with 1×10^5 $CD3^+$ T cells, and changes in cortical bone mass were quantified in the femoral diaphysis by high-resolution (6 μm) μCT, in cross-sectional groups at 6, 9, 14, and 20 months of age. (A) Cortical indices are as follows: cortical thickness and cortical area. Data are expressed as mean ± standard error of the mean: $*P < .05$ and $**P < .01$ for T cell compared with sham by 2-way analysis of variance with Bonferroni posttest. Nonsignificant comparisons not shown. n = 12 mice/group at 6 months, 20–22 mice/group at 9 months, 15–16 mice/group at 14 months, and 15–16 mice/group at 20 months. (B) Representative high-resolution (6 μm) 3-dimensional reconstructions of femoral cortical bone for sham and reconstituted (T cells) mice at baseline (6 months) and 9, 14, and 20 months of age. Scale bars represent 500 μm.

(Figure 2A). Representative 3-dimensional reconstructions of femoral cortical bone are shown in Figure 2B.

Bone Histomorphometry Reveals Increased Osteoclast Indices in 20 Month-Old T-Cell Reconstituted Mice

Quantitative bone histomorphometry was used to assess dynamic and/or static changes in bone formation and resorption at 20 months of age in the trabecular compartment of the femur. Compared to sham mice, the number of osteoclasts normalized for bone surface, and surfaces covered by osteoclasts, were significantly elevated in T-cell reconstituted mice (Figure 3A). Representative images of TRAP staining for osteoclasts (red cells) are shown in Figure 3B.

The key dynamic indices of bone formation (bone formation rate and mineral apposition rate) were not significantly different between groups (Figure 3C). Representative images of calcein double-labeled bone surfaces are shown in Figure 3D.

Changes in Biochemical Indices of Bone Turnover and Osteoclastogenic Cytokines in Reconstituted Mice

Serum biochemical markers of bone turnover were quantified in control (sham) and T-cell reconstituted mice (T cells) cross-sectionally at baseline (6 months), 12 weeks after reconstitution (9 months of age), and at 14 and 20 months of age (Figure 4A).

Two-way ANOVA revealed significant effects of time ($P < .0001$), but not of T-cell reconstitution or interaction between time and T cells, on serum CTx, a marker of bone resorption (Figure 4A). The CTx was significantly elevated in T-cell reconstituted mice due to IRBL at 9 months of age (3 months after transplant) but not at other time points.

Likewise, 2-way ANOVA revealed significant effects of time ($P = .0018$) but not T-cell reconstitution, or interaction between time and T-cells, on serum osteocalcin, a bone formation marker. There were also no differences between sham and T cell-reconstituted groups at any time point (Figure 4A).

To better understand the underlying drivers of bone resorption, we further quantified serum concentrations of RANKL, the key osteoclastogenic cytokine, and of OPG, its physiological moderator, and we derived a RANKL/OPG ratio that better reflects the net state of RANKL activity in the body (Figure 4B and C).

RANKL showed significant effects of time ($P = .0008$) and T-cell reconstitution ($P < .0001$) but without significant interaction between time and T cells. Osteoprotegerin showed significant effects of time ($P < .0001$) but not of T-cell reconstitution or interaction between time and T cells. After deriving a RANKL/OPG ratio, both time ($P = .0278$) and T-cell reconstitution ($P = .0002$) were significant but not interaction.

Relative to sham mice, RANKL was significantly elevated 3 months after immune reconstitution (9 months of age) and remained significantly elevated at 14 and 20 months of

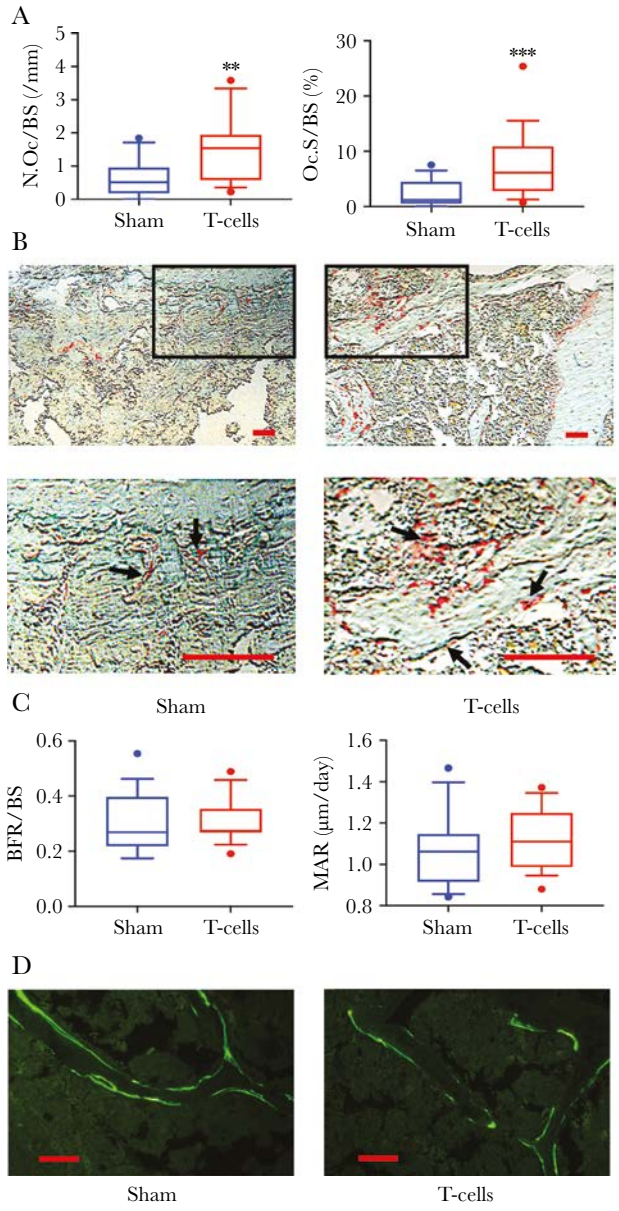

Figure 3. Histomorphometry of sham and T-cell reconstituted (T cells) mice at 20 months of age. Six-month-old female TCRβ knockout (KO) mice were sham-reconstituted (Sham) or T-cell reconstituted by adoptive transfer with 1×10^5 $CD3^+$ T cells, and changes in static and/or dynamic histomorphometric indices were quantified in the trabecular compartment of the femur at 20 months of age. (A) Number of osteoclasts normalized for bone surface (N.Oc/BS) and surfaces covered by osteoclasts normalized for bone surface (Oc.S/BS). (B) Representative images of tartrate-resistant acid phosphatase (TRAP) staining for osteoclasts (red cells) in sham and T-cell reconstituted mice (T cells). Images at the top are presented at ×200 final magnification, and images at the bottom represent boxed regions scaled to ×800. Black arrows designate osteoclasts and red scale bars = 100 µm. (C) Dynamic bone formation indices: bone formation rate normalized for bone surface (BFR/BS) and mineral apposition rate (MAR). (D) Representative images of calcein double labeling are shown for sham and T-cell reconstituted mice (T cells). Images taken with a ×20 objective (×200 final magnification) and red scale bars = 100 µm. Data are expressed as boxplots (median ± interquartile range) with 10 to 90 percentile whiskers: $^{**}P < .01$ and $^{***}P < .001$ by Student's *t* test (N.Oc/BS and MAR) or Mann-Whitney *U* test (Oc.S/BS and BFR/BS). Nonsignificant comparisons not shown. n = 15–16 mice/group.

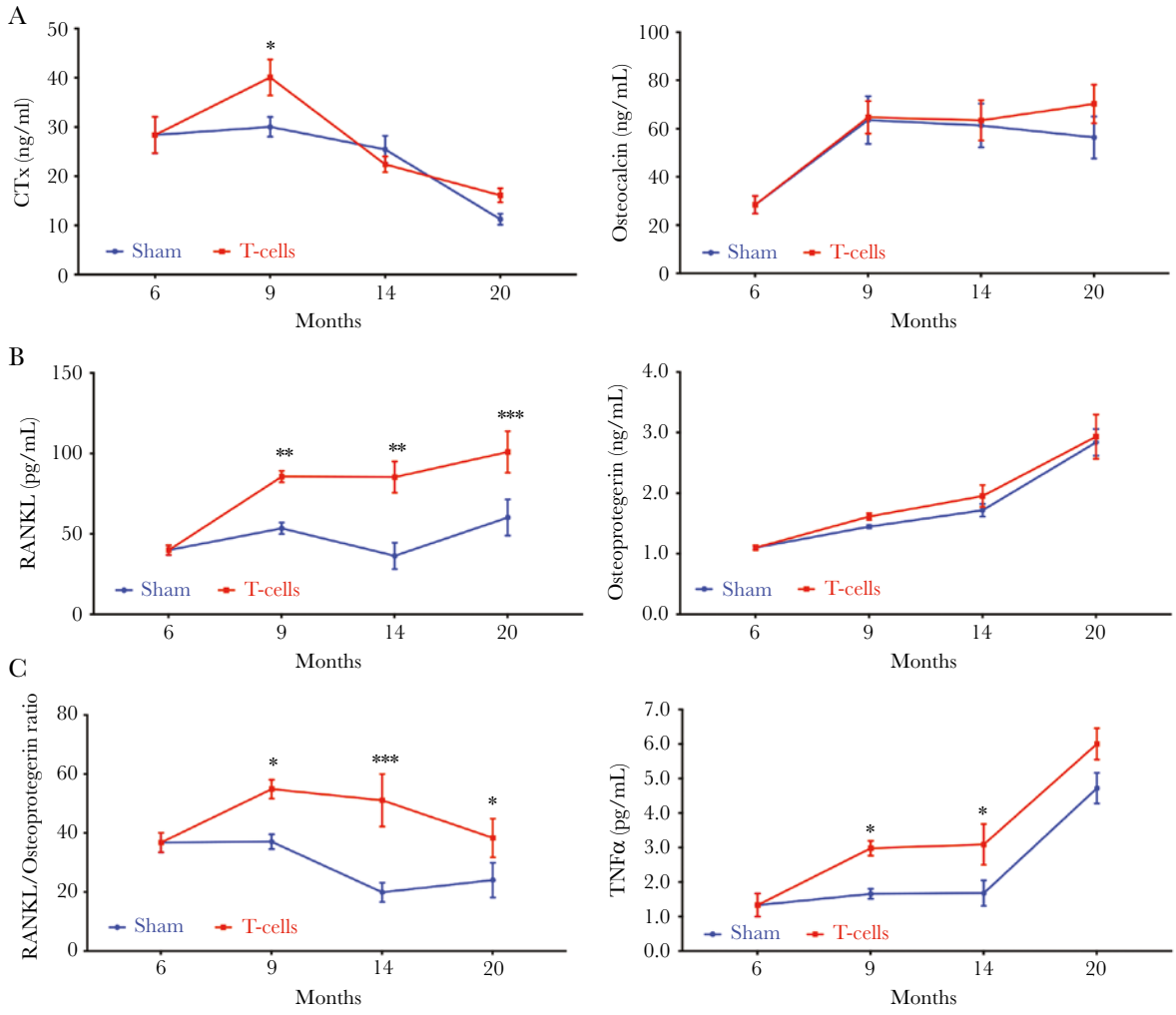

Figure 4. Serum biochemical indices of bone turnover and circulating osteoclastogenic mediators in sham and T-cell reconstituted mice (T cells). Circulating mediators were quantified in sham- and T-cell reconstituted mice in cross-sectional groups at baseline (6 months) and 9, 14, and 20 months of age. (A) Serum biochemical markers of bone turnover, C-terminal telopeptide of type I collagen (CTx), and osteocalcin. (B) Osteoclastogenic mediators RANKL, and osteoprotegerin and (C) the derived RANKL/osteoprotegerin ratio, and the inflammatory/osteoclastogenic effector tumor necrosis factor (TNF)α. Data are expressed as mean ± standard error of the mean: $*P < .05$, $**P < .01$, and $***P < .001$ for T cell compared with sham by 2-way analysis of variance with Bonferroni posttest. Nonsignificant comparisons not shown. n = 8 mice/group at 6 months, 20–23 mice/group at 9 months, 15–16 mice/group at 14 months, and 10–16 mice/group at 20 months.

age (Figure 4B). Osteoprotegerin was not significantly different between sham and reconstituted mice at any time point (Figure 4B), which accounted for an imbalance in the RANKL/osteoprotegerin ratio and is propitious for continued bone resorption. We further quantified TNFα, a potent inflammatory cytokine that promotes RANKL and amplifies RANKL activity to enhance osteoclastogenesis and bone resorption [8].

Two-way ANOVA revealed significant effects of time ($P < .0001$) and T-cell reconstitution ($P = .0018$) but no significant interaction between time and T cells. The increase in TNFα concentrations with time (age) is consistent with the known development of an inflammatory state in aging humans and rodents that has been hypothesized to contribute to age-associated bone loss [34]. Relative to sham, TNFα was significantly elevated in T-cell reconstituted mice 3 months after transplant and at 14 months of age but not at 20 months of age (Figure 4C).

These data suggest that trabecular bone resorption is the major mechanism accounting for both IRBL and age-associated bone loss and is driven by inflammatory cytokines including RANKL and TNFα.

Reconstituted CD4$^+$ T Cells Are a Significant Source of Osteoclastogenic Cytokines in Aging Mice

We have previously reported that the reconstituted CD4$^+$ T cells are a major source of RANKL and TNFα, which drive both trabecular and cortical IRBL [28, 29]. To assess the contribution of reconstituted CD4$^+$ T cells to bone loss in aging mice, we immunomagnetically purified CD4$^+$ T cells from reconstituted mice and performed gene expression analysis for

key inflammatory genes, using NanoString nCounter mRNA quantification. Because untransplanted TCRβ KO mice lack T cells, we used 20-month-old WT C57BL6/J mice as a reference. The data (Figure 5A and B) revealed significantly elevated expression of *Rankl and Tnf*, whereas expression of the gene for osteoprotegerin (*Tnfsf11b*) was very low in $CD4^+$ T cells but increased significantly in reconstructed mice (Figure 5A). We further derived a RANKL/osteoprotegerin ratio (Figure 5A), which was significantly elevated, suggesting that the small, albeit significant, increase in osteoprotegerin expression was unable to fully compensate for the increase in RANKL, skewing the balance in favor of increased osteoclastogenesis.

It is interesting to note that *Il1β* (Figure 5B) and *Il17a* (Figure 5C) gene expressions were also significantly elevated in $CD4^+$ T cells from reconstituted mice, whereas $CD4^+$ T-cell expression of *IL6* transcript was low and did not change significantly between groups (Figure 5C).

Taken together, the μCT data reveal that although cortical IRBL in young animals is temporary and does not further complicate cortical bone loss caused by aging, trabecular IRBL was permanent and cumulative, leading to exacerbated trabecular bone loss in old animals. Histomorphometry further revealed expanded osteoclast numbers in the trabecular bone of old reconstituted animals, whereas bone formation indices were unaffected. These data were consistent with significantly elevated

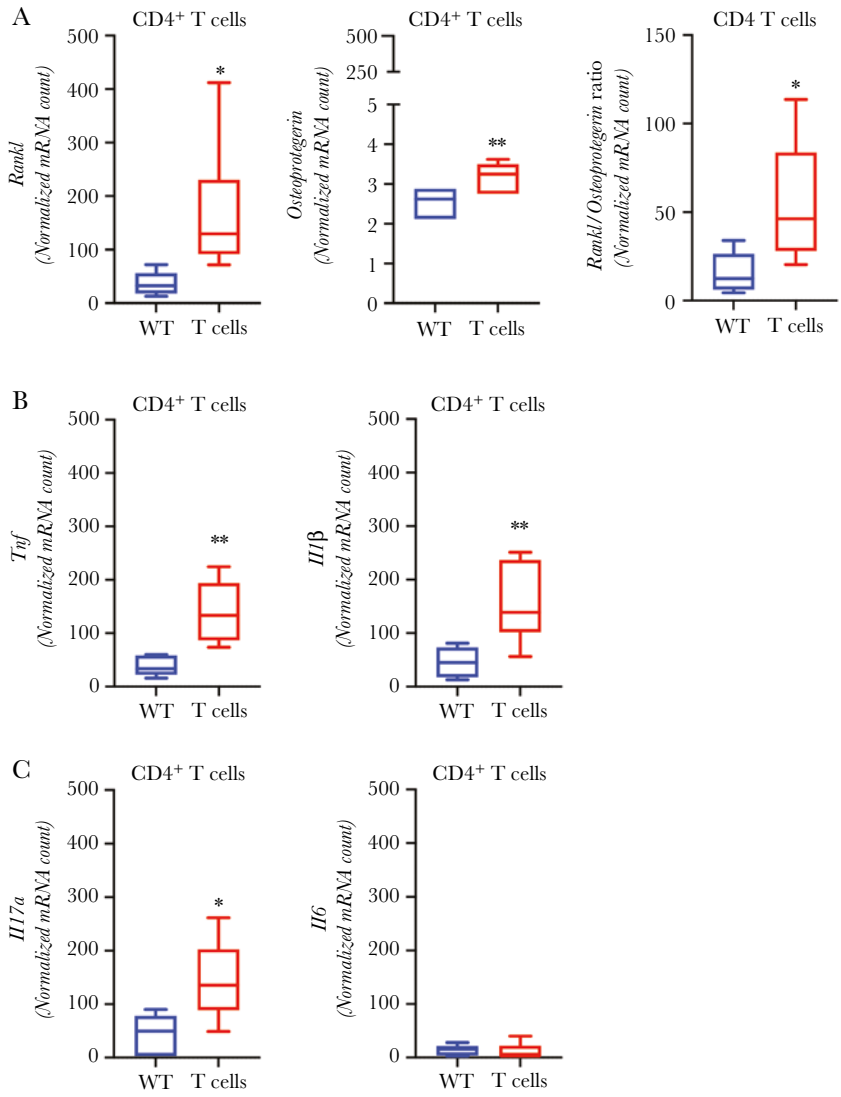

Figure 5. Quantification of gene expression patterns of inflammatory and osteoclastogenic cytokines in purified $CD4^+$ T cells in mice at 20 months of age. $CD4^+$ T cells were immunomagnetically purified from spleens of 20-month-old wild-type (WT) C57BL6/J and T-cell-reconstituted TCRβ knockout (KO) mice (T cells) and subjected to NanoString mRNA gene quantification for common osteoclastogenic and inflammatory cytokines: (A) mRNA for downstream osteoclastogenic mediators (RANKL, osteoprotegerin, and the RANKL/osteoprotegerin ratio). (B) Inflammatory mediators of osteoclastogenesis (tumor necrosis factor [TNF]α and IL-1β) and (C) IL-17A and IL-6. Data are expressed as boxplots (median ± interquartile range) with 10 to 90 percentile whiskers: $*P < .05$ and $**P < .01$ by Mann-Whitney *U* test. Nonsignificant comparisons not shown. n = 5 WT and 7 T-cell mice/group.

serum RANKL in 20-month-old mice, whereas osteoprotegerin, a RANKL decoy receptor and resorption inhibitor, did not differ between sham and T-cell reconstituted groups, leading to a net RANKL/osteoprotegerin ratio that remained elevated in reconstituted mice into old age. Increased osteoclast indices were further consistent with elevated expression of osteoclastogenic cytokines by $CD4^+$ T cells in old mice, including increased expression of RANKL, IL-1β, IL-17A, and TNFα. These data suggest an important ongoing contribution of reconstituted $CD4^+$ T cells to the trabecular bone resorption associated with aging.

DISCUSSION

There is concern that HIV/ART-induced bone loss may collide with aging bone loss in PWH, culminating in an epidemic of fractures and offsetting the gains in patient health that have been achieved through the advent of ART itself [35, 36]. It is now established that ART-induced bone loss is relatively transient, occurring mainly within the first 6 months after ART initiation and with bone resorption then remitting [37]. Because most patients are relatively young when first initiating ART, it is possible that ART-induced IRBL in younger PWH is regenerated over time through bone remodeling, a bone renewal/repair program in rodents and humans. Whether this occurs or not is unknown, and with this uncertainty there has been little impetus to treat patients initiating ART prophylactically, to prevent IRBL, or to treat low BMD in PWH early, to prevent fractures in later life.

Although certain ART drugs directly induce modest bone loss (typically 1%–2%) [38], many PWH suffer intense ART-induced bone loss that is independent of regimen [22–26]. Indeed, even with more modern ART regimens, including tenofovir alafenamide and integrase strand inhibitor-based ART, bone loss may still persist, with some PWH sustaining ≥4% BMD loss [39]. We have proposed that immune reconstitution downstream of ART-induced viral suppression may account for the bone loss that occurs independent of specific ART formulation [26], and we have developed an animal model of IRBL [28] to further investigate IRBL mechanisms and actions on bone.

In the present study, our data reveal that, as with humans, IRBL in young adult mice is transient (~3 months in mice and then plateaus). However, IRBL in the trabecular compartment of both the axial and appendicular skeletons was permanent and not reversed through bone remodeling. Furthermore, the convergence of IRBL and age-associated trabecular bone loss was cumulative and led to an exaggerated loss of bone volume by 20 months, an age considered old in mice [31]. The data were consistent with elevated osteoclast numbers and increased osteoclastic cytokine production by $CD4^+$ T cells at 20 months, suggesting that the homeostatically expanded T cells remained inherently hyperresponsive throughout life.

By contrast, whereas cortical bone parameters were significantly diminished after 3 months of IRBL, they recovered thereafter and were no longer significantly different in 20-month-old mice, although a trend to decreasing bone mass was observed that could eventually become significant again at advanced age.

As expected, cortical bone mass continued to accrue with age in the long bones of mice, and, similar to humans, the cortical compartment of long bones continues to increase in cortical area due to periosteal apposition, increasing the diameter of the bone. By contrast, cortical thickness declines with age due to endocortical bone resorption of the endosteal surface, resulting in thinner bones and a widening of the bone marrow cavity.

It is interesting to note that CTx was only significantly different between groups during the 3 months of intense IRBL and then declined to control levels. However, CTx fell with age in both groups possibly due to reduced basal turnover in older mice. Nevertheless, because changes in CTx reflect predominantly cortical bone resorption, the lack of differences at 14 and 20 months is consistent with the muted changes observed in cortical μCT indices at these time points, despite continuing loss of trabecular bone. This may further explain why CTx did not reflect the serum changes in RANKL and TNFα beyond the IRBL period. Indeed, aggressive bone loss was observed in the cortical compartment during the first 3 months of IRBL, and this was reflected by increases in CTx.

Although osteoprotegerin did not differ between sham and T-cell reconstituted groups, it did climb significantly with age, a phenomenon that has also been reported in human studies [40, 41] and has been suggested to represent a possible homeostatic mechanism to limit bone loss [40]. The fact that osteoprotegerin did not differ between groups suggests that increased RANKL and TNFα are the dominant drivers of bone resorption and that osteoprotegerin acts, in part, to offset age-associated bone loss but not IRBL. However, the persistent rise in osteoprotegerin with age may have served to partially ameliorate the excessive bone resorption driven by IRBL, accounting for the plateauing of bone resorption at 14 months and consistent with the RANKL/osteoprotegerin ratio that was biased in favor of RANKL and ongoing bone resorption. However, serum osteoprotegerin (and other serum factors) is representative of production across the total organism and may not accurately reflect local production at sites of bone turnover.

Why $CD4^+$ T cells produce heightened levels of osteoclastogenic cytokines during aging is unclear. However, expansion of T cells from a modest pool may lead to a contraction of the T-cell repertoire and accumulation of T-cell clones responding aggressively to foreign and self-antigens. Such reactive T-cell populations could mediate a persistent inflammatory response, which is indeed a well documented feature of PWH on long-term ART [36]. A similar effect is observed in aging and is referred to as "inflammaging" due to age-associated

contraction of the T-cell repertoire leading to accumulation of autoreactive T cells [42]. Our mouse model may be replicating these events, although the antigens involved are presently unclear. Interleukin-17A, whose production we found to be increased in $CD4^+$ T cells, is a key product of $CD4^+$ Th17 cells. Th17 cells are potently osteoclastogenic because they directly secrete RANKL and TNFα as well as IL-17A, a cytokine that induces RANKL production by cells of the osteoblast lineage. It is interesting to note that in healthy mice, the major source of Th17 cells is the gut, where they form in response to specific antigens, in mice, specifically those from segmented filamentous bacteria [43], which are ubiquitous in the environment, although more than 20 bacterial strains in humans have been reported to be capable of inducing Th17 formation when transplanted into mice [44].

We have previously reported that $CD4^+$ T cells drive aggressive cortical and trabecular IRBL; however, $CD8^+$ T cells may also contribute to trabecular bone loss [29]. Consequently, there may be additional contributions from $CD8^+$ T cells and other adaptive immune components that respond to $CD4^+$ T cells, including B cells and macrophages, further adding to bone loss in aging.

Study Limitations

Mice may not accurately model mice do not accurately model all aspects of bone loss in humans and do not model the direct effects on bone of some antiretroviral agents [45] or the direct effects of breakthrough HIV replication on osteoclasts [46].

CONCLUSIONS

In conclusion, our data show that although cortical bone may regenerate in part, IRBL in the trabecular compartment is permanent and is cumulative with age-associated bone loss later in life. The loss of trabecular bone has consequences for bone strength and may contribute to higher fracture rates in PWH, leading to detrimental outcomes for long-term health and wellbeing. If the mouse data are replicated in humans, prophylactic interventions to prevent bone loss may be warranted, including administration of antiosteoporotic pharmaceuticals such as zoledronic acid, which can prevent ART-induced bone loss during the early stages of ART initiation [13, 37].

Notes

Acknowledgments. We thank Penny Roon and the Augusta University Electron Microscopy and Histology Core Laboratory for preparation of histological sections for histomorphometry. We also thank the San Francisco VA Health Care System/University of California, San Francisco Skeletal Biology and Biomechanics Core (supported by AR066262) for performing NanoString mRNA quantification.

Authorship contributions. M. N. W. and I. O. designed the studies. M. N. W. analyzed the data and wrote the manuscript. D. W., T. V., S. R.-P., K. Y., M. E. M.-L., C.-L. T., and W. C. performed the studies. All authors reviewed the manuscript.

Disclaimer. The content is solely the responsibility of the authors and does not represent the official views of the National Institutes of Health or the Department of Veterans Affairs.

Financial support. Research reported in this publication was funded by the National Institute of Arthritis and Musculoskeletal and Skin Diseases under Award Numbers AR068157, AR070091 and AR079298 (to M. N. W. and I. O.). M. N. W. and I. O. are also funded in part by a grant from the National Institute on Aging (NIA) under Award Number AG062334, and M. N. W. is funded by a grant from the Biomedical Laboratory Research & Development Service (BLR&D) of the VA Office of Research and Development (BX000105). W. C. is supported by grants from BLR&D Grants BX005851, BX004813, and BX004835. M. E. M.-L. was funded by Grant AG036675 from the NIA.

Potential conflicts of interest. All authors: No reported conflicts of interest. All authors have submitted the ICMJE Form for Disclosure of Potential Conflicts of Interest.

References

1. Guaraldi G, Orlando G, Zona S, et al. Premature age-related comorbidities among HIV-infected persons compared with the general population. Clin Infect Dis **2011**; 53:1120–6.
2. Moran CA, Weitzmann MN, Ofotokun I. Bone loss in HIV infection. Curr Treat Options Infect Dis **2017**; 9:52–67.
3. Bolland MJ, Grey A. HIV and low bone density: responsible party, or guilty by association? IBMS BoneKEy **2011**; 8:7–15.
4. Titanji K, Ofotokun I, Weitzmann MN. Immature/transitional B-cell expansion is associated with bone loss in HIV-infected individuals with severe CD4+ T-cell lymphopenia. AIDS **2020**; 34:1475–83.
5. Titanji K, Vunnava A, Foster A, et al. T-cell receptor activator of nuclear factor-kappaB ligand/osteoprotegerin imbalance is associated with HIV-induced bone loss in patients with higher CD4+ T-cell counts. AIDS **2018**; 32:885–94.
6. Titanji K, Vunnava A, Sheth AN, et al. Dysregulated B cell expression of RANKL and OPG correlates with loss of bone mineral density in HIV infection. PLoS Pathog **2014**; 10:e1004497.
7. Vikulina T, Fan X, Yamaguchi M, et al. Alterations in the immuno-skeletal interface drive bone destruction in HIV-1 transgenic rats. Proc Natl Acad Sci USA **2010**; 107:13848–53.
8. Weitzmann MN, Ofotokun I. Physiological and pathophysiological bone turnover - role of the immune system. Nat Rev Endocrinol **2016**; 12:518–32.
9. Tebas P, Powderly WG, Claxton S, et al. Accelerated bone mineral loss in HIV-infected patients receiving potent antiretroviral therapy. AIDS **2000**; 14:F63–7.

10. Stellbrink HJ, Orkin C, Arribas JR, et al. Comparison of changes in bone density and turnover with abacavir-lamivudine versus tenofovir-emtricitabine in HIV-infected adults: 48-week results from the ASSERT study. Clin Infect Dis **2010**; 51:963–72.
11. McComsey GA, Tebas P, Shane E, et al. Bone disease in HIV infection: a practical review and recommendations for HIV care providers. Clin Infect Dis **2010**; 51:937–46.
12. Hansen AB, Obel N, Nielsen H, Pedersen C, Gerstoft J. Bone mineral density changes in protease inhibitor-sparing vs. nucleoside reverse transcriptase inhibitor-sparing highly active antiretroviral therapy: data from a randomized trial. HIV Med **2011**; 12:157–65.
13. Ofotokun I, Titanji K, Lahiri CD, et al. A single-dose zoledronic acid infusion prevents antiretroviral therapy-induced bone loss in treatment-naive HIV-infected patients: a phase IIb trial. Clin Infect Dis **2016**; 63:663–71.
14. Triant VA, Brown TT, Lee H, Grinspoon SK. Fracture prevalence among human immunodeficiency virus (HIV)-infected versus non-HIV-infected patients in a large U.S. healthcare system. J Clin Endocrinol Metab **2008**; 93:3499–504.
15. Young B, Dao CN, Buchacz K, Baker R, Brooks JT. Increased rates of bone fracture among HIV-infected persons in the HIV outpatient study (HOPS) compared with the US general population, 2000-2006. Clin Infect Dis **2011**; 52:1061–8.
16. Womack JA, Goulet JL, Gibert C, et al. Increased risk of fragility fractures among HIV infected compared to uninfected male veterans. PLoS One **2011**; 6:e17217.
17. Sharma A, Shi Q, Hoover DR, et al. Increased fracture incidence in middle-aged HIV-infected and HIV-uninfected women: updated results from the women's interagency HIV study. J Acquir Immune Defic Syndr **2015**; 70:54–61.
18. Guerri-Fernandez R, Vestergaard P, Carbonell C, et al. HIV infection is strongly associated with hip fracture risk, independently of age, gender, and comorbidities: a population-based cohort study. J Bone Miner Res **2013**; 28:1259–63.
19. Prieto-Alhambra D, Guerri-Fernandez R, De Vries F, et al. HIV infection and its association with an excess risk of clinical fractures: a nationwide case-control study. J Acquir Immune Defic Syndr **2014**; 66:90–5.
20. Ofotokun I, Weitzmann MN. HIV and bone metabolism. Discov Med **2011**; 11:385–93.
21. Ofotokun I, McIntosh E, Weitzmann MN. HIV: inflammation and bone. Curr HIV/AIDS Rep **2012**; 9:16–25.
22. Bruera D, Luna N, David DO, Bergoglio LM, Zamudio J. Decreased bone mineral density in HIV-infected patients is independent of antiretroviral therapy. AIDS **2003**; 17:1917–23.
23. Tebas P, Umbleja T, Dube MP, et al. Initiation of ART is associated with bone loss independent of the specific ART regimen: results of ACTG A5005s. In: 14th Conference on Retroviruses and Opportunistic Infections, Los Angeles, CA, 25–28 February 2007.
24. Brown TT, McComsey GA, King MS, Qaqish RB, Bernstein BM, da Silva BA. Loss of bone mineral density after antiretroviral therapy initiation, independent of antiretroviral regimen. J Acquir Immune Defic Syndr **2009**; 51:554–61.
25. Piso RJ, Rothen M, Rothen JP, Stahl M. Markers of bone turnover are elevated in patients with antiretroviral treatment independent of the substance used. J Acquir Immune Defic Syndr **2011**; 56:320–4.
26. Ofotokun I, Titanji K, Vunnava A, et al. Antiretroviral therapy induces a rapid increase in bone resorption that is positively associated with the magnitude of immune reconstitution in HIV infection. AIDS **2016**; 30:405–14.
27. Grant PM, Kitch D, McComsey GA, et al. Low baseline CD4+ count is associated with greater bone mineral density loss after antiretroviral therapy initiation. Clin Infect Dis **2013**; 57:1483–8.
28. Ofotokun I, Titanji K, Vikulina T, et al. Role of T-cell reconstitution in HIV-1 antiretroviral therapy-induced bone loss. Nat Commun **2015**; 6:8282.
29. Weitzmann MN, Vikulina T, Roser-Page S, Yamaguchi M, Ofotokun I. Homeostatic expansion of CD4+ T cells promotes cortical and trabecular bone loss, whereas CD8+ T cells induce trabecular bone loss only. J Infect Dis **2017**; 216:1070–9.
30. Wing EJ. HIV and aging. Int J Infect Dis **2016**; 53:61–8.
31. Flurkey K, Currer JM, Harrison DE. The mouse in aging research. In: Fox JG, Barthold S, Davisson M, Newcomer CE, Quimby FW, Smith A, eds. The Mouse in Biomedical Research. 2nd ed. Vol. 1-4: Elsevier; **2007**: pp 637–72.
32. Roser-Page S, Vikulina T, Zayzafoon M, Weitzmann MN. CTLA-4Ig-induced T cell anergy promotes Wnt-10b production and bone formation in a mouse model. Arthritis Rheumatol **2014**; 66:990–9.
33. Weitzmann MN, Roser-Page S, Vikulina T, et al. Reduced bone formation in males and increased bone resorption in females drive bone loss in hemophilia A mice. Blood Adv **2019**; 3:288–300.
34. Lencel P, Magne D. Inflammaging: the driving force in osteoporosis? Med Hypotheses **2011**; 76:317–21.
35. Amorosa V, Tebas P. Bone disease and HIV infection. Clin Infect Dis **2006**; 42:108–14.
36. Deeks SG, Tracy R, Douek DC. Systemic effects of inflammation on health during chronic HIV infection. Immunity **2013**; 39:633–45.
37. Ofotokun I, Collins LF, Titanji K, et al. Antiretroviral therapy-induced bone loss is durably suppressed by a single dose of zoledronic acid in treatment-naive persons with HIV infection: a phase IIB trial. Clin Infect Dis **2020**; 71:1655–63.

38. Moran CA, Weitzmann MN, Ofotokun I. The protease inhibitors and HIV-associated bone loss. Curr Opin HIV AIDS **2016**; 11:333–42.
39. Sax PE, Wohl D, Yin MT, et al. Tenofovir alafenamide versus tenofovir disoproxil fumarate, coformulated with elvitegravir, cobicistat, and emtricitabine, for initial treatment of HIV-1 infection: two randomised, double-blind, phase 3, non-inferiority trials. Lancet **2015**; 385:2606–15.
40. Khosla S, Arrighi HM, Melton LJ 3rd, et al. Correlates of osteoprotegerin levels in women and men. Osteoporos Int **2002**; 13:394–9.
41. Indridason OS, Franzson L, Sigurdsson G. Serum osteoprotegerin and its relationship with bone mineral density and markers of bone turnover. Osteoporos Int **2005**; 16:417–23.
42. Goronzy JJ, Weyand CM. Aging, autoimmunity and arthritis: T-cell senescence and contraction of T-cell repertoire diversity - catalysts of autoimmunity and chronic inflammation. Arthritis Res Ther **2003**; 5:225–34.
43. Ivanov II, Atarashi K, Manel N, et al. Induction of intestinal Th17 cells by segmented filamentous bacteria. Cell **2009**; 139:485–98.
44. Tan TG, Sefik E, Geva-Zatorsky N, et al. Identifying species of symbiont bacteria from the human gut that, alone, can induce intestinal Th17 cells in mice. Proc Natl Acad Sci USA **2016**; 113:E8141–50.
45. DeJesus E, Ramgopal M, Crofoot G, et al. Switching from efavirenz, emtricitabine, and tenofovir disoproxil fumarate to tenofovir alafenamide coformulated with rilpivirine and emtricitabine in virally suppressed adults with HIV-1 infection: a randomised, double-blind, multicentre, phase 3b, non-inferiority study. Lancet HIV **2017**; 4:E205–13.
46. Raynaud-Messina B, Bracq L, Dupont M, et al. Bone degradation machinery of osteoclasts: An HIV-1 target that contributes to bone loss. Proc Natl Acad Sci USA **2018**; 115:E2556–65.